Sulfoxide, sulfur, and nitrogen oxidation and dealkylation by cytochrome P450

Rydberg, Patrik; Ryde, Ulf; Olsen, Lars

Published in:
Journal of Chemical Theory and Computation

DOI:
10.1021/ct800101v

2008

Document Version:
Peer reviewed version (aka post-print)

Sulfoxide, sulfur, and nitrogen oxidation and dealkylation by cytochrome P450

Patrik Rydberg,† Ulf Ryde,‡ Lars Olsen†*

Contribution from Department of Medicinal Chemistry, Copenhagen University, Universitetsparken 2, DK-2100 Copenhagen, Denmark, and the Department of Theoretical Chemistry, Lund University, P.O.B 124, SE-22100 Lund, Sweden

E-mail: lo@farma.ku.dk

RECEIVED DATE (to be automatically inserted after your manuscript is accepted if required according to the journal that you are submitting your paper to)

Hetero-atom oxidation and dealkylation by Cytochrome P450

† Copenhagen University ‡ Lund University

The oxidation and dealkylation of dimethylsulfoxide (DMSO), dimethylsulfide (DMS), and trimethylamine (TMA) by cytochrome P450 have been studied with density functional theory calculations. The results show that the oxidation reactions always occur on the doublet spin surface, whereas dealkylations can take place for both the doublet and quartet spin states. Moreover, DMS is more reactive than DMSO, and S-oxidation is more favorable than S-dealkylation, whereas N-dealkylation is more favorable than N-oxidation. This is in perfect

agreement with experimental results, showing that density functional activation energies are reliable and comparable for widely different reactions with cytochrome P450.

Introduction

The cytochromes P450 (CYPs) constitute an enzyme family that is found in all types of organisms, from bacteria to mammals. In the human genome, there are 57 genes for CYPs.[1] These isoforms have functions including synthesis and degradation of many physiologically important compounds, as well as degradation of xenobiotic compounds, e.g. drugs.[2] Numerous studies have been performed on these enzymes, because they influence the transformation of pro-drugs into their active form as well as the bioavailability and degradation of many drugs. In fact, it has been estimated that the CYPs are responsible for ~75% of the phase I metabolism of drugs.[3]

The active site in the CYPs is buried inside the protein and connected to the surface by several channels, which vary between the various isoforms.[4,5] At the bottom of the active site, there is a heme group with a central iron ion. Below the plane of the heme group, the sulfur atom of a cysteine amino acid coordinates to the iron ion, whereas the site above the heme plane may bind various extraneous small ligands during the reaction cycle. In the resting state, this position is occupied by a water molecule.

The CYPs catalyze several different types of reactions, of which the most common ones are hydroxylation of saturated C–H bonds, dealkylations, epoxidation of double bonds, oxidation of aromatic ring systems, and oxidation of hetero atoms. Most of these reactions, have been thoroughly characterized using theoretical calculations,[6,7] but hetero-atom oxidation has been much less studied than the other types of reactions.[8-12] The active species in the reactions is in general a high-valent (formally Fe^{V}=O) state of the active-site heme group, called compound I. It has two close-lying electronic states, a doublet and a quartet, and they may contribute

differently to various reactions. For example, they give comparable activation energies for aliphatic hydroxylation, whereas the addition of compound I to the aromatic ring system is most favorable on the doublet spin surface.[6,7]

For substrates containing hetero atoms, there is the possibility of both hetero-atom oxidation and dealkylation, as is shown in Scheme 1. The dealkylation reaction starts with hydroxylation of the C^{α} atom, followed by a cleavage of the bond between the heteroatom and C^{α}. Interestingly, N-containing compounds seem to prefer the hydroxylation–dealkylation reaction, whereas the opposite is true for S-containing compounds.[9,13-16] It is a challenge for theoretical methods to explain these trends. Loew and Chang[6] have addressed this question using Hartree–Fock calculations but they could rationalize the experimental observations only if they used different criteria for different reactions: The relative stability of the oxidation products could explain why N-compounds prefer dealkylation. However, to explain the preference for oxidation of S-compounds, they instead had to compare the energy difference between the C^{α} radical intermediate and the sulfoxide products. In this paper, we try to obtain a consistent view of the N-, S-, and SO-oxidation and dealkylation reactions by using more accurate density functional theory (DFT) calculations. We study the substrates trimethylamine (TMA), dimethylsulfide (DMS), and dimethylsulfoxide (DMSO). To our best knowledge, this is the first time sulfoxide oxidation and dealkylation are studied by DFT calculations.

Scheme 1. The reaction paths of hetero-atom oxidation (Ox) and hetero-atom dealkylation (D-a).

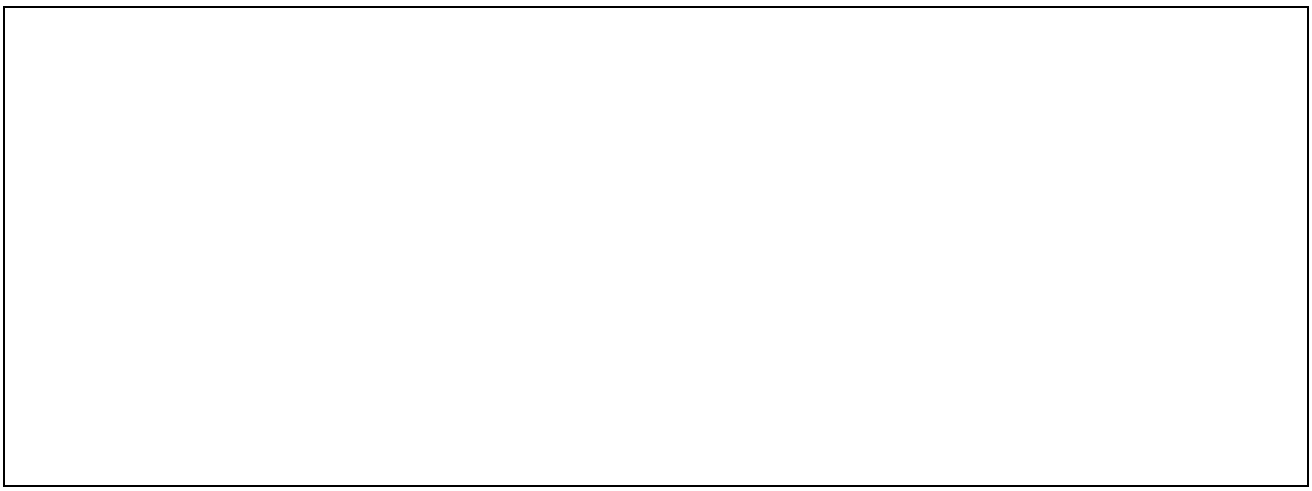

Computational Methodology

We have modeled the compound I species of the CYPs as iron (formally Fe^{V}) porphine (i.e. a porphyrin without side chains), with CH_3S^- and O^{2-} as axial ligands. Four different states along the reactions were studied (Scheme 1), viz. compound I and substrate isolated from each other, the complex between compound I and substrate (the reactant complex, **R**), the transition state (**TS**), and the product after the oxidation (**P**^{Ox}) or the intermediate after the dealkylation (**I**$^{D-a}$; cf. Scheme 1). All energies are given relative to that of the reactant complex (**R**). All four states were studied in both the doublet and quartet states.

The quantum chemical calculations were performed with the density functional method B3LYP[17-19] with the VWN(V) correlation functional[20] (unrestricted formalism for open shell systems). In the geometry optimizations, we used for iron the double-ζ basis set of Schäfer et al.,[21] enhanced with a *p* function with the exponent 0.134915. For the other atoms, the 6-31G(d) basis set[22-24] was used (this combination is denoted BSI). More accurate energies were determined by single-point calculations at the B3LYP/6-311++G(2d,2p) level[25] with the double-ζ basis set of Schäfer et al.,[21] enhanced with *s*, *p*, *d*, and *f* functions (exponents of 0.01377232, 0.041843, 0.1244, 2.5, and 0.8; two *f* functions) on iron[26] (denoted BSII). The

B3LYP functional was chosen because it has previously been shown to give very good geometries compared to crystal structures, as well as energies, compared to CCSD(T) and CASPT2 calculations for heme models.[27,28] Moreover, it has been employed in almost all recent studies of CYP reactions.[6,7,29]

To get a view of what effects a surrounding protein may have on these reactions we have performed calculations in vacuum, as well as with an implicit solvent model (note that the CYPs are a large enzyme family,[1] so it is not possible to model the general effect of the protein in a more detailed way). The effective dielectric constant (ε) in proteins has been much discussed, and values from 2 to 40 have been suggested.[30-32] Therefore, we tested three different values, 1, 4, and 80, to get a feeling of possible effects of the protein. Solvent calculations were carried out at the B3LYP/BSI level with the continuum conductor-like screening model (COSMO).[33] For the atomic radii, we used the optimized COSMO radii in Turbomole[34] (and 2.0 Å for Fe). For all the other parameters, we employed the default values, implying a water-like probe molecule. The full data are presented in Table S1 in the supporting information. They show that the continuum solvent stabilizes the separated reactants relative to the reactant complex by 9–11 and 16–20 kJ/mol for ε = 4 and 80, respectively. The two spin states are always affected in the same way for both spin states, so the solvent gives no net effect on the spin splitting energy. The solvent effect on the activation energies depends on the substrate, but not on the reaction type: For DMSO the activation energies increase by 3–7 kJ/mol, for DMS they are not much affected ($\pm$2 kJ/mol), whereas for TMA they decrease by 5–9 kJ/mol (with ε = 4; ε= 80 gives similar, but larger effects, up to 18 kJ/mol). Thus, possible solvation effects of the enzyme will not change the general conclusions of this paper, regarding the relative activation energies of the oxidation and dealkylation reactions and the

three types of substrates.

Frequency calculations were performed at the B3LYP/BSI level of theory to obtain the zero-point vibrational energy and thermal corrections to the Gibbs free energy (at 298 K and 1 atm pressure, using an ideal-gas approximation[35]). They also verified that the structures represent true minima or transition states. All calculations were carried out with the Turbomole program package, version 5.9.[36] Presented energies are those obtained at the B3LYP/BSII level, including the zero-point vibrational energy, thermal corrections to the Gibbs free energy, and solvent effects with a dielectric constant of 4. The charges and spin densities presented were calculated with Mulliken population analysis in vacuum.

Previous studies of sulfur and nitrogen oxidation[8,10-12] used a SH^- model of the cysteine iron ligand, instead of our CH_3S^- model (which is the preferred cysteine model in the theoretical study of all other proteins). Therefore, we studied the difference between these two models for the DMS oxidation. These studies were restricted to the quartet spin state, because we failed to locate the doublet transition state with the SH^- model. The two models gave very similar geometries, with differences of 0.005, 0.008, and 0.004 Å for the Fe–O distance, 0.056, 0.003, and 0.008 Å for the Fe–S_{Cys} distance, and 0.009, 0.013, and 0.001 Å for the O–S_{DMS} distance for the reactant complex, the transition state, and the product complex, respectively. The only significant geometric difference was that the two models sometimes gave different C/H_{Cys}–S_{Cys}–Fe–N torsion angles, owing to differing interactions between the methyl group or the hydrogen atom of the cysteine model and the porphyrin ring. The CH_3S^- model gave a 12 kJ/mol higher activation energy and a 14 kJ/mol less negative energy of the product, but the energetic effects of solvation, zero-point vibrational energies, and basis set changes were very similar and always of the same sign. We also calculated the structure of compound I with the

SCH_3^- and SH^- models in both the doublet and quartet spin states. Again, the geometries were very similar and the energy splitting between the two spin states differed by less than 0.3 kJ/mol. The full data of this comparison is presented in Tables S2 and S3 in the supporting information.

We also tested the effect of amide NH···S_{Cys} interactions in the protein by single-point energy calculations with two added NH_3 groups at the B3LYP/BSI level, as has been done by Ogliaro et al.[37] However, we found that the energies from such calculations are unreliable, because the differences in the C/H_{Cys}–S_{Cys}–Fe–N torsions and the S_{Cys}–Fe–N angles between the reactions and between the various states in the same reaction give varying interactions between the NH_3 groups and the porphyrin ring. Therefore, these results are not presented.

Results and Discussion

Hetero-atom oxidation by cytochrome P450 may occur via direct O-atom transfer or an initial electron-transfer from the substrate to compound I, followed by the formation of a bond between the hetero atom and the oxygen atom.[2,6] However, we have only studied the former reaction, because experimental results have shown that this is the most likely reaction for sulfoxidation,[38] and previous theoretical investigations have given the same results for both sulfoxidation and nitrogen oxidation.[8-10]

DMSO oxidation and dealkylation. Sulfoxides are important groups in drugs and have therefore been thoroughly studied experimentally.[39] They are also interesting because any oxidation of a sulfide can be followed by a second oxidation of the sulfoxide, resulting in a sulfone. Neither sulfoxide oxidation nor dealkylation seems to have been studied before with theoretical methods. We find that the reactant complex of DMSO and compound I is 28–29

kJ/mol less stable than the isolated substrate and compound I for both the doublet and quartet states (owing to solvation effects and the loss in translational and rotational entropy). The oxidation transition state displays a relatively large splitting (13 kJ/mol) between the doublet (73 kJ/mol) and quartet (86 kJ/mol) states, showing that this reaction is more likely to take place on the doublet spin surface (cf. Figure 1). This is also reflected in the transition-state geometries: The doublet has an early transition state with an S–O distance of 2.11 Å, whereas the quartet transition state is late with an S–O distance of 1.94 Å (cf. Figure 2).

Next, we turn to the dealkylation reaction of DMSO. The activation energies for the hydrogen abstraction step in this reaction display a similar but opposite splitting (9 kJ/mol) between the doublet and quartet states (Figure 1). This difference is caused entirely by the thermal corrections; without them, the difference is only 1 kJ/mol. Moreover, the activation energy is larger for the hydroxylation reaction than for the direct oxidation of DMSO, and the hydroxylation reaction is more likely to occur on the quartet spin surface (91 kJ/mol). The geometries of the transition states are much more similar than in the oxidation reaction. The quartet transition state is only slightly later than the doublet with O-H distances of 1.13 and 1.17 Å, respectively.

There are two possible conformations of the DMSO molecule in the dealkylation reaction: The oxygen atom in DMSO can either point towards or away from the heme ring. However, the reactant state with the oxygen atom pointing towards heme is 14 kJ/mol less stable than the other conformation. On the other hand, the two conformations gave similar transition-state structures with similar energies for the quartet spin state and only a 6 kJ/mol difference in doublet spin state. Energies for the less stable conformation are shown in Table S4 in the supporting information.

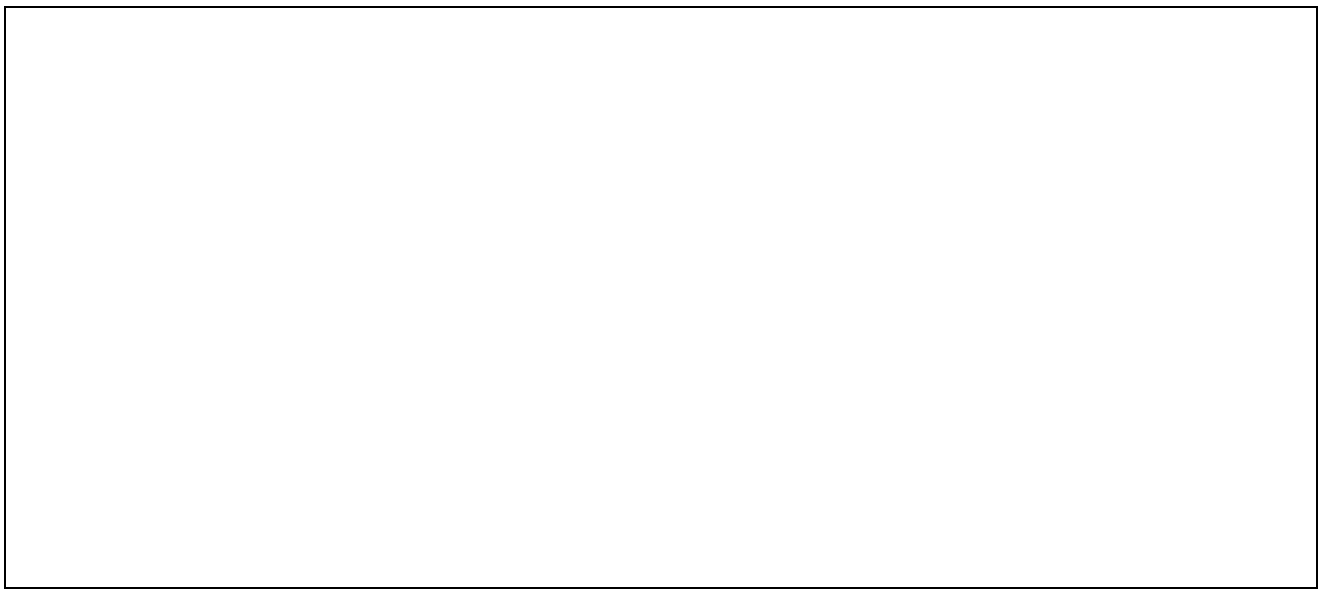

Figure 1. Relative energies (in kJ/mol) for the various states in the reactions with DMSO.

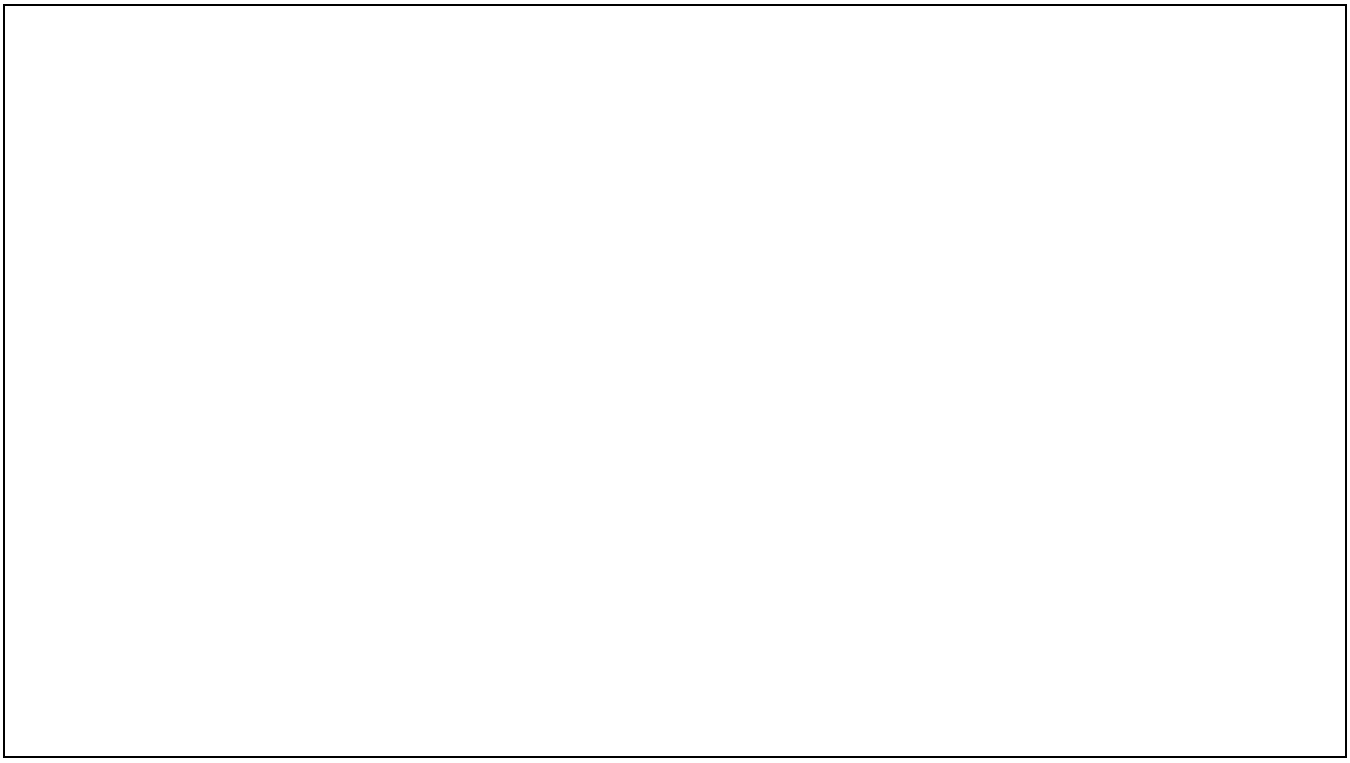

Figure 2. Structures of the various states in the DMSO reactions. Data are given for the doublet (quartet) spin state with distances in Å and angles in degrees. Imaginary frequencies for the transition states are shown on the lower right side of the respective structure.

DMS oxidation and dealkylation. Sulfide reactions are important reactions in drug metabolism by cytochrome P450.[13,14] They have been studied theoretically before,[8-10,12,40] (but only the quartet spin state for the dealkylation reaction). The oxidation of DMS is similar to the oxidation of DMSO: The doublet state has lower activation energy (47 kJ/mol) than the quartet state (63 kJ/mol, cf. Figure 3). Thus, the activation energy of the doublet state is 25 kJ/mol lower than that for the DMSO oxidation. This is also reflected in the transition-state structure, in which the S–O distance is 2.22 Å for the doublet (Figure 4), i.e. an earlier transition state than that of the sulfoxide oxidation. Moreover, the reactant complex is 41–42 kJ/mol higher in energy than the separated substrate and compound I.

In contrast to DMSO, the activation energy of the DMS dealkylation reaction is lower on the doublet surface (64 kJ/mol) than on the quartet surface (75 kJ/mol, Figure 3). Thus, they are higher than the activation energy for the direct S-oxidation reaction, but lower than those of the corresponding dealkylation step for DMSO. The intermediate in the dealkylation reaction, $\mathbf{I}^{\mathbf{D\text{-}a}}$, is also ~30 kJ/mol more stable than for DMSO. This is because the sulfur atom in DMS has one more available orbital available to accommodate the substrate radical that is formed in this state.

Figure 3. Relative energies (in kJ/mol) for the various states in the reactions with DMS.

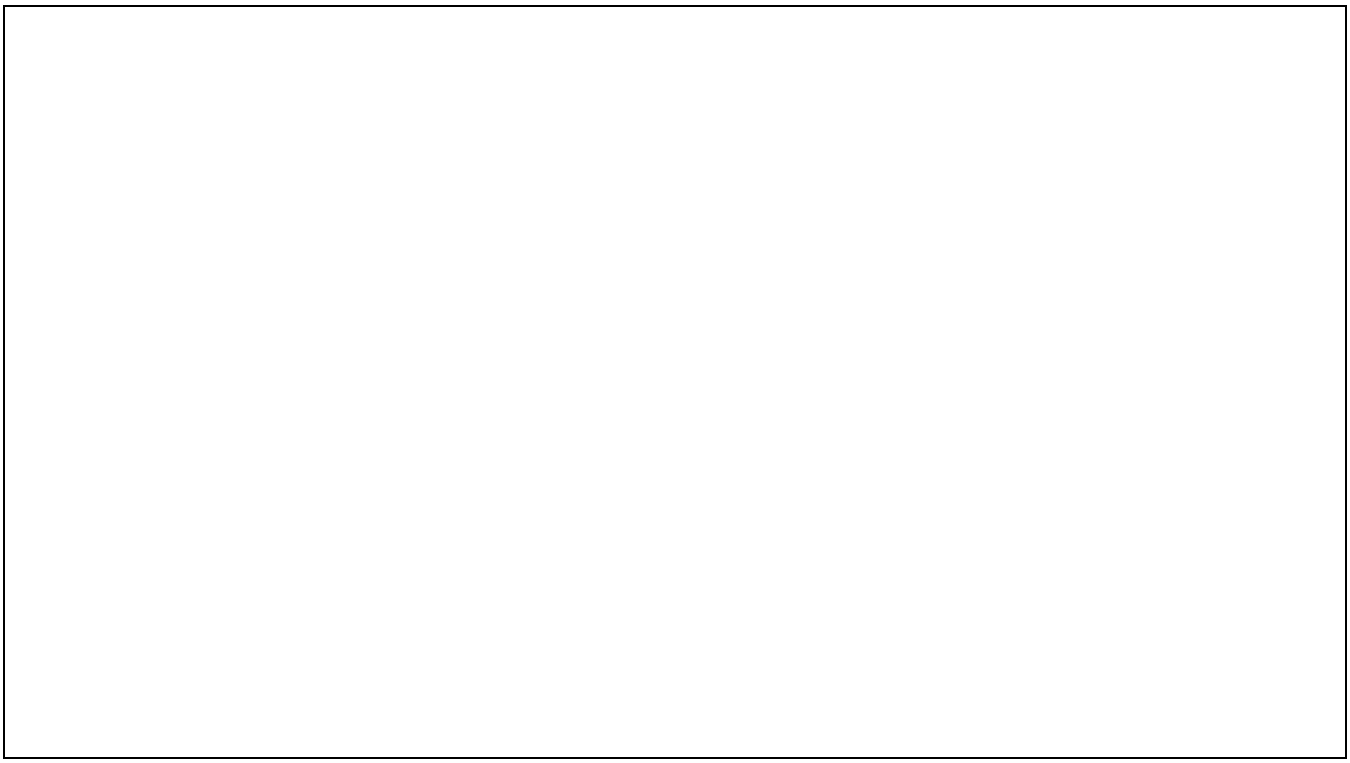

Figure 4. Structures of the various states in the DMS reactions. Data are given for the doublet (quartet) spin state with distances in Å and angles in degrees. Imaginary frequencies for the transition states are shown on the lower right side of the respective structure.

TMA oxidation and dealkylation. Most drugs contain nitrogen atoms, which often are metabolized by cytochrome P450. Experimentally, it is found that dealkylation is preferred before N-oxidation.[16] The dealkylation reaction (caused by hydroxylation of the C^{α} atom) has been the subject of several theoretical investigations,[9,11,40,41] but the N-oxidation has only been studied once before with DFT,[11] viz. for the substrate *N*,*N*-dimethylaniline. Here, we study the dealkylation and N-oxidation reactions for a simpler substrate, TMA, and compare them to the corresponding reactions with DMS and DMSO.

Our results show that the reactant complex is 44–45 kJ/mol less stable than the separated substrate and compound I for both spin states. The activation energy for TMA oxidation is 53

kJ/mol on the doublet surface, but significantly higher for the quartet, 75 kJ/mol (cf. Figure 5). This is also reflected in the transition-state geometries: The doublet has an early transition state with an O–N distance of 2.02 Å, whereas the quartet transition state is late, with an O–N distance of 1.82 Å (Figure 6).

For the corresponding dealkylation reaction, the activation energies of the doublet and quartet differ by 5 kJ/mol, with that of the doublet state having the smaller barrier of 35 kJ/mol. This is lower than the N-oxidation reaction.

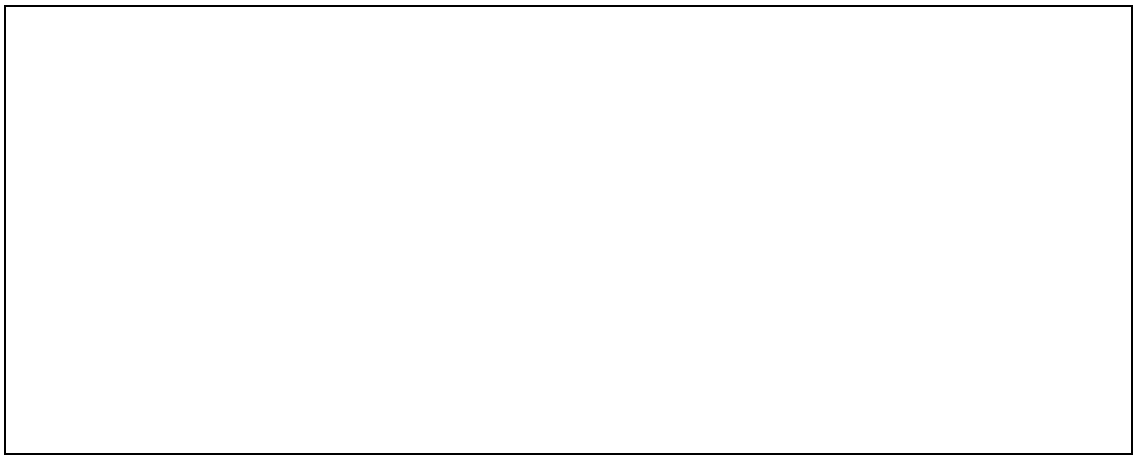

Figure 5. Relative energies (in kJ/mol) for the various states in the reactions with TMA. No energy is given for $^{2}I^{D\text{-}a}$, because this state converges directly to the hydroxylated product complex.

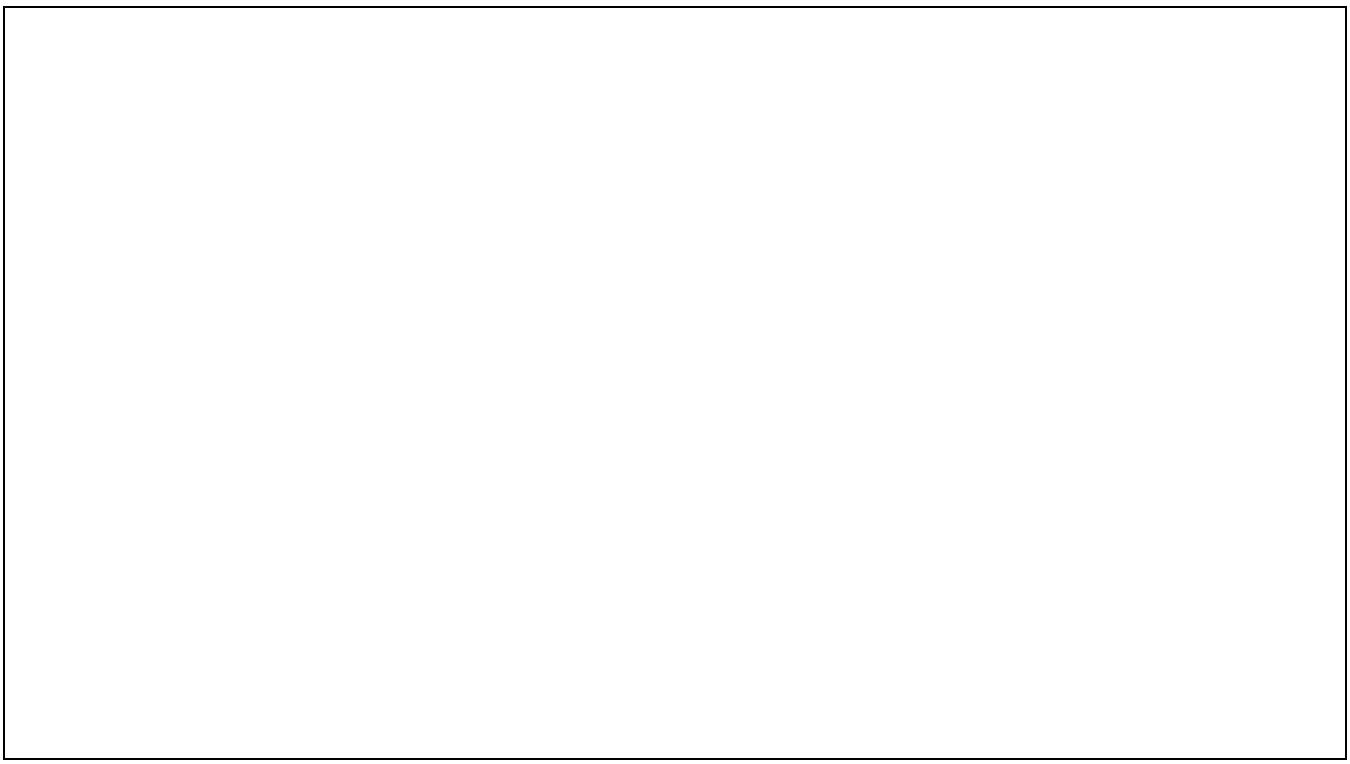

Figure 6. Structures for the various states in the TMA reactions. Data are given for the doublet (quartet) spin state with distances in Å and angles in degrees. Imaginary frequencies for the transition states are shown on the lower right side of the respective structure.

Comparison with experimental data. Our results for the hetero-atom oxidation and dealkylation reactions suggest that sulfides and sulfoxides are more likely to undergo hetero-atom oxidation than dealkylation, because the S- and SO-oxidation activation energies are 16–18 kJ/mol lower than that for the corresponding dealkylation reaction. Of course, the reactivity will depend on the properties of the enzyme pocket and the substituents on the substrate, but our results agree well with the experimental observation that CYPs in general degrade S-containing compounds by S-oxidation rather than by dealkylation.[9,13-16] It has also been noted that CYPs perform sulfoxidation faster than sulfoxide oxidation.[39] This is in perfect agreement with the 25 kJ/mol lower activation energy for DMS oxidation than for DMSO oxidation (12

kJ/mol from the isolated reactants).

There is a similar difference in the activation energies between the N-oxidation and N-dealkylation reactions (19 kJ/mol). However, in contrast to the S-containing compounds, the N-dealkylation reaction has lower activation energy than the N-oxidation. This suggests that the N-dealkylation reactions are more likely to occur (especially as different N-compounds all give similar hydroxylation barriers[40]), again in excellent agreement with experiments.[9,13-16]

Rationalization of the trends. The dealkylation reactions have activation energies ranging from 35 (TMA) to 100 (DMSO) kJ/mole. This large variation can be explained by the ability of the substrate to stabilize the radical that is formed during the reaction. If we plot the percentage of the spin of the substrate on the carbon from which the hydrogen is abstracted against the activation energy, we get correlation coefficients (r^2) of 0.96 or 0.99 for the final free energies or the raw BSI energies as is shown in Figure 7 (the zero-point and thermal corrections lower the correlation somewhat). Thus, it is clear that the type of neighboring atom (i.e. the possibility to delocalize the radical over several atoms) strongly affects the activation energy of the dealkylation reactions, as has been shown before in a different manner.[40]

For the oxidation reactions, the variation of the activation energies between the three substrates is much smaller: For the doublet state, the activation energies are 48–73 kJ/mol relative to the **R** complex, but 89–101 kJ/mol relative to the isolated reactants. Thus, there hardly any trends to explain.

On the other hand, the preference for the double state of the oxidation reactions can be easily rationalized: Previous DFT studies have shown that compound I essentially contains three unpaired electrons, one localized on the iron ion, one on the oxy group, and one shared by the porphyrin ring and the cysteine model.[6,7,29] In the quartet state, all three spins are

parallel, whereas in the doublet state, the latter spin is antiparallel to the other two. Our calculated spin densities in Tables S8–S10 in the supporting information confirm this also for the present calculations. In the hetero-atom oxidation, two electrons with opposite spin in the same orbital are moved from the substrate to compound I. In the doublet state, this is straight forward, because the two acceptor orbitals (one on the oxy group and the other shared by the porphyrin ring and the cysteine model) are singly occupied with electrons of opposite spins (cf. Scheme 2). However, for the quartet state, the two acceptor orbitals have parallel spin and one of the electrons must either flip spin or end up in another orbital (an unoccupied iron 3*d* orbital), giving an excited product state.

This is reflected in the spin densities (Tables S8–S10): The doublet transition state has only a small spin on the substrate (~0.1 *e* for DMSO and ~0.3 *e* for the other two substrates), whereas the more spin is found on the substrate in the quartet state (~0.5 *e*). Moreover, the spin on the iron ion has increased in the quartet state. This shows that one of the electrons goes mainly to iron, rather than to the oxy group. Consequently, the $^{2}\mathbf{P}^{ox}$ state is always a pure low-spin Fe(III) state, with essentially no spin on the substrate. However, the quartet $^{4}\mathbf{P}^{ox}$ state contains intermediate-spin Fe(III) state (with three unpaired electrons), with 0.2–0.4 unpaired electrons on the cysteine model, but no spin on the product (including the former oxy group). This shows that one electron has also moved from a doubly occupied Fe orbital to the oxy group.

For the hydroxylation reaction, no such differences arise, because the intermediate involves a radical, which will have the same spin as the unpaired electron in the porphyrin ring in compound I.

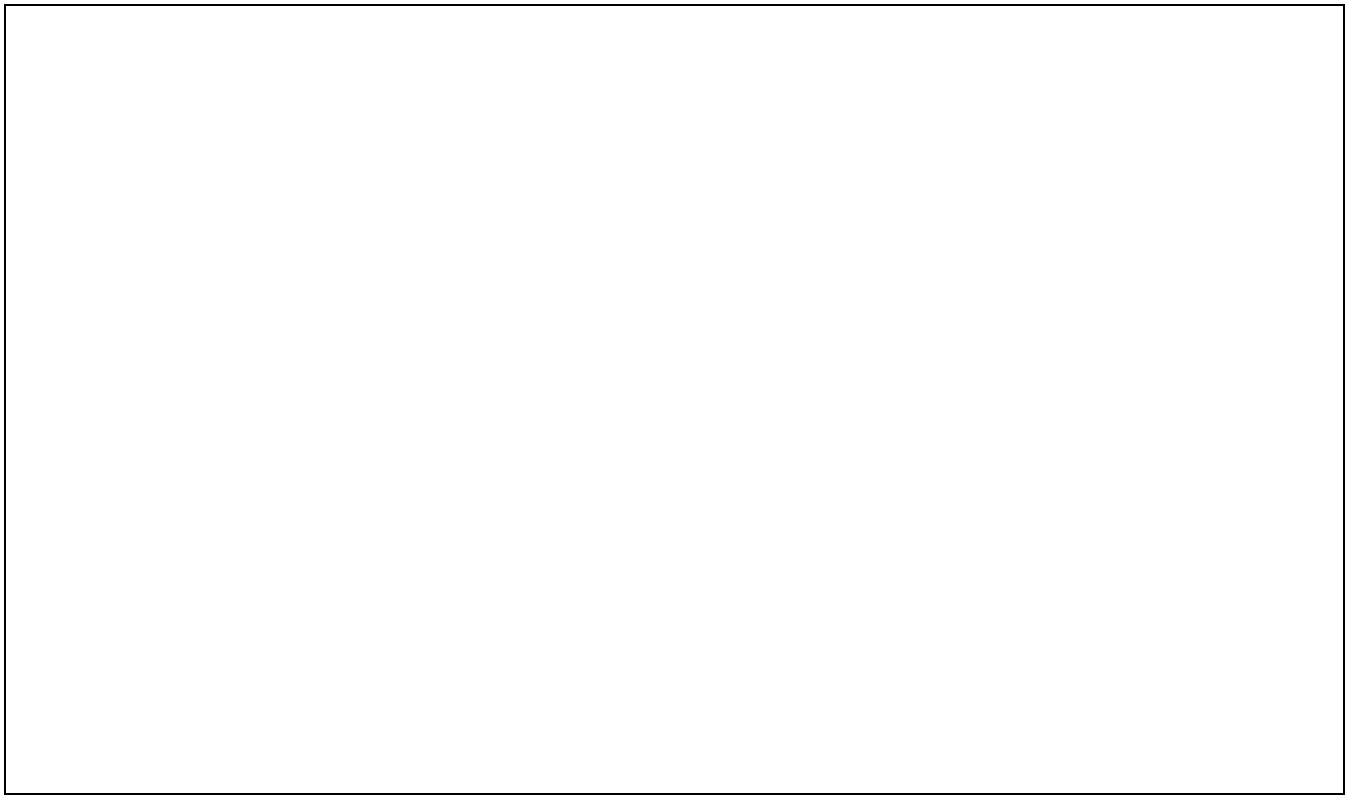

Figure 7. The correlation between the activation energy of the dealkylation reactions and the percentage of the substrate spin that resides on the carbon atom from which the hydrogen atom is abstracted. The red squares represent the final energies and the blue triangles represent the BSI energy.

Scheme 2. Schematic picture of the movement of electrons in the hetero-atom oxidation reaction in the doublet and quartet states.

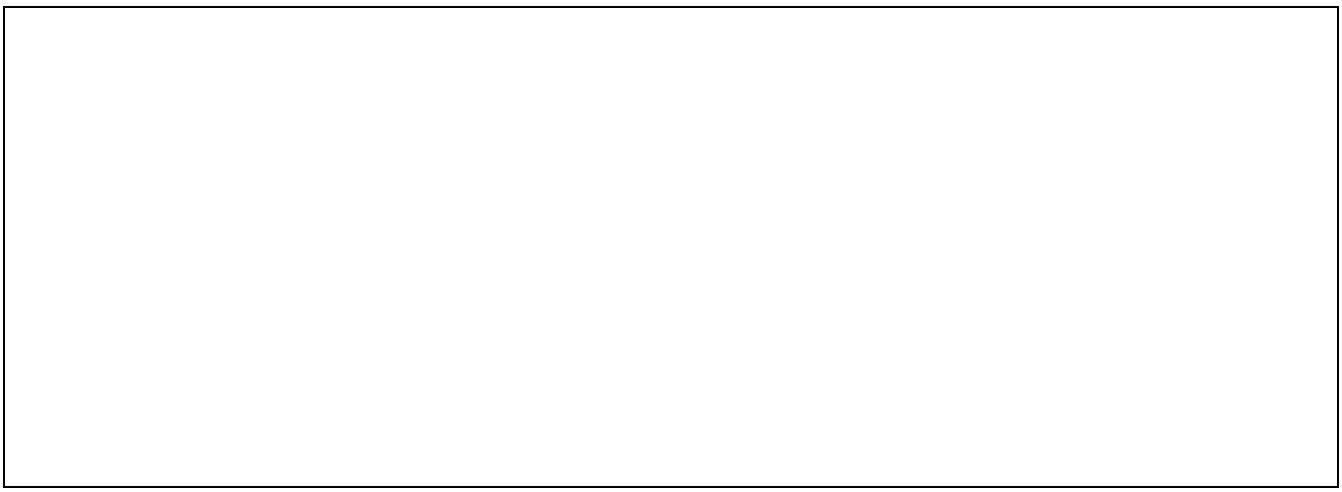

Comparison with previous studies. As mentioned above, the nitrogen oxidation by cytochrome P450 has only been studied once before,[11] with the substrate *N*,*N*-dimethylaniline. These results are quite similar to ours (disregarding the thermal corrections, which were not included in the other study). For example, the Fe–O and O–N distances for oxidation transition states differ by less than 0.03 Å between *N*,*N*-dimethylaniline and TMA (distances for the dealkylation transition state were not given[11]). For the activation energies of the two reactions and the two spin states, the differences are somewhat larger, 4–12 kJ/mol, but not larger than what could be expected from the differences in details of the calculations (especially the cysteine model) and the fact that different substrates were studied.

The oxidation of DMS has previously been studied by Shaik and coworkers[8,10,12] The two earlier studies[8,10] suggested the reaction to take place on the quartet spin surface, with a quite high activation energy. However, these results were recently revised and a new and lower transition state on the doublet spin surface was presented.[12] Energetically, our results agree quite well with the latter results (again disregarding the thermal corrections and also the amide hydrogen-bond model): Their activation energies are 29 and 43 kJ/mol for the doublet and quartet, respectively which is reasonably close to our energies of 32 and 55 kJ/mol,

considering the difference in the cysteine model. The transition-state structures of the quartet states are also quite similar, with differences of 0.02–0.04 Å for the S–O, Fe–O, and Fe–S distances and 3° for the Fe–O–S angle. Likewise, the imaginary frequencies agree within 9 cm^{-1}.

However, some discrepancies are observed for the doublet transition state: Shaik and coworkers observe a S–O distance of 2.39 Å, a Fe–O distance of 1.66 Å and an imaginary frequency of 1015 *i* cm^{-1}, whereas we get a S–O distance of 2.22 Å, a Fe–O distance of 1.72 Å and a much smaller imaginary frequency of 61 *i* cm^{-1}. Therefore, we performed scans of the O–S distance for the DMS oxidation (and also TMA and DMSO oxidation for comparison, Figure S2 in the supporting information). These showed a very flat potential surface, explaining our low frequencies. Moreover, we also scanned the Fe–O distance for several different O–S distances around the transition state for the DMS oxidation. This two-dimensional surface is shown in Figure 8 and confirms the flat potential energy surface. We also analyzed the eigenmode of our transition state and confirmed that it corresponds to the correct reaction coordinate (shown in Figure S1 in the supporting information). Moreover, we have also tried to locate the transition state reported by Shaik and coworkers by restrained optimizations, using both SCH_3^- and SH^- as the cysteine model. However, we always found a low imaginary frequency (less than 100 *i* cm^{-1}) and when removing the restraints, the geometry converged back to the structure shown in Figure 4. To understand the difference between our calculations we finally optimized the transition state, with SH^- as the cysteine model, using the LACVP** basis set[42] and the Jaguar software[43] (version 7.0; Shaik and coworkers used this basis set and Jaguar 6.5), as well as with the Turbomole software.[36] The results show geometries in between our geometry and the one they have found (as shown in Figure 8), with

Fe–O distances of 1.69 and 1.68 Å, and O–S distances of 2.28 and 2.31 Å with the Jaguar and Turbomole software, respectively. The imaginary frequencies of these two structures were 124 and 291 *i* cm^{-1}. Therefore, we conclude that the two structures most likely represent the same transition state, but the flat potential surface makes it extremely sensitive to variations in the theoretical method. However, it should be characterized by a low imaginary frequency; the frequency reported by Shaik and coworkers is much too large for a reaction involving only heavy atoms, especially on this flat potential surface.

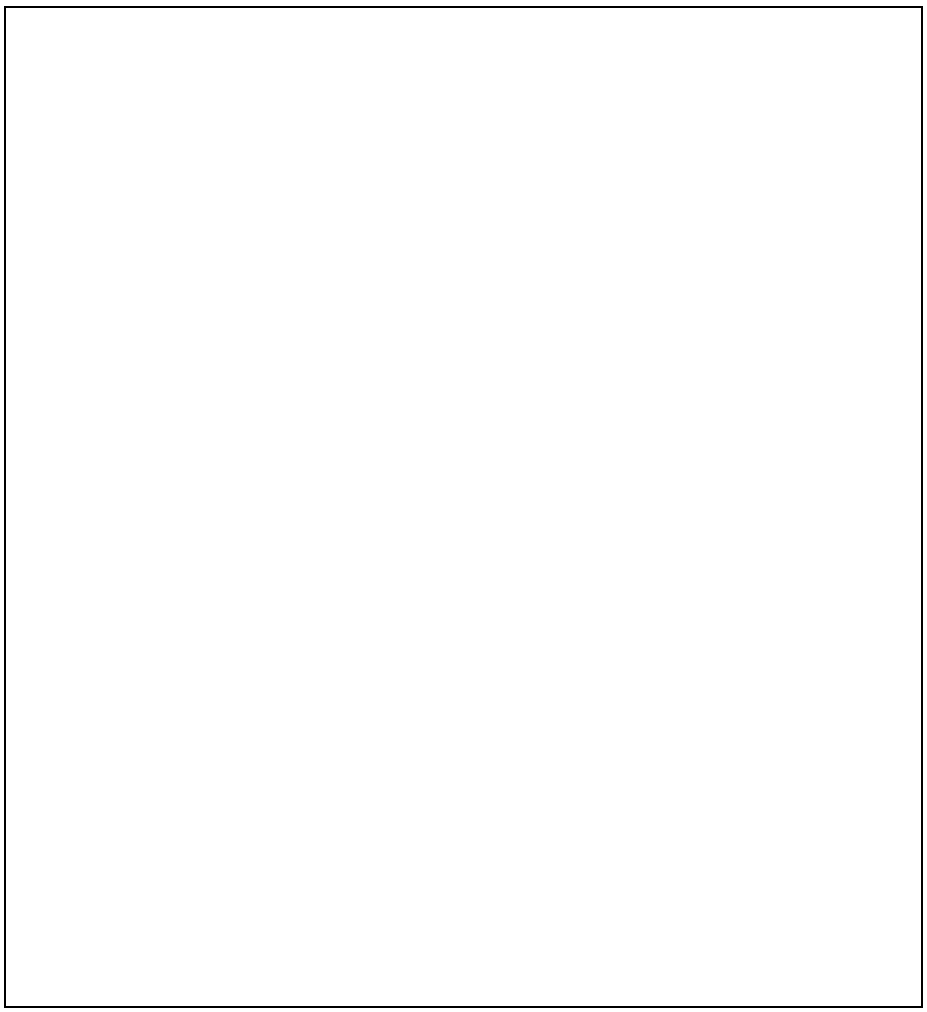

Figure 8. Scatter plot of the energies around the transition state of the DMS oxidation reaction in the doublet spin state. The points are color coded according to the energies computed with BSI in kJ/mol. The geometries of the transition state calculated with B3LYP/LACVP** and by

Shaik et al. are shown as black stars. The reactant state has been excluded from the figure to make it clearer. It has a S–O distance of 4.14 Å, and a Fe–O distance of 1.63 Å.

Conclusions

We have studied the oxidation and dealkylation of DMSO, DMS, and TMA with the same DFT approach to obtain a consistent view of these six reactions. The results clearly show that for sulfur and sulfoxide compounds, hetero-atom oxidation is the preferred pathway (the activation energies for the oxidations of DMSO and DMS are 73 and 47 kJ/mol, respectively, whereas the activation energies for the corresponding dealkylations are 91 and 64 kJ/mol) and it will always take place on the doublet spin surface. For nitrogen-containing compounds, on the other hand, the dealkylation has lower activation energy than the oxidation, 35 and 53 kJ/mol, respectively. The results do not change if possible solvent effects in the protein are considered. These results are in excellent agreement with the experimental findings that S-oxidation is more favorable than S-dealkylation, that N-dealkylation is more favorable than N-oxidation, and that hetero-atom oxidation is more common for S- than for N-containing molecules.[9,13-16] Moreover, the barrier for DMS oxidation is lower than that for DMSO oxidation, again in agreement with experiments.[39]

Thus, our results rationalize all experimental findings using a single criterion, viz. the activation energy for the various reactions, calculated at the DFT level. This is a most important finding, because it shows that the calculated activation energies are consistent and comparable also for different types of reactions. This is mandatory for a predictive method of the intrinsic reactivity of an arbitrary drug candidate with cytochromes P450. Previous methods, based on semiempirical calculations, have had severe problems in this respect.[41]

Thus, our calculations indicate that it may be possible to estimate the intrinsic reactivity of any reaction for a drug candidate with DFT methods, and therefore probably also by other, cheaper theoretical methods,[40] an important goal in medicinal chemistry.

Acknowledgement. This work was supported by grants from the Carlsberg Foundation, the Benzon Foundation, and the Swedish Research Council. It has also been supported by computer resources from Lunarc at Lund University.

Supporting Information Available: Comparison of the SCH_3^- and SH^- cysteine models. Energies for the dealkylation of DMSO with the alternative conformation. All energy data for the reactions. Charge and spin distributions of all states studied. Figure of the eigenmodes of the DMS transition state in the doublet spin state. Figures of the S–O or N–O distance scans for all three substrates. Figures of the highest occupied natural orbitals in all the transition states studied.

Reference List

1. Guengerich, F. P. Human Cytochrome P450 Enzymes. In *Cytochrome P450 Structure, Mechanism, and Biochemistry*, 3 ed.; Ortiz de Montellano, P. R., Ed.; Kluwer Academic / Plenum Publishers: New York, 2004; pp 377-531.
2. Guengerich, F. P. Common and uncommon cytochrome P450 reactions related to metabolism and chemical toxicity. *Chem. Res. Toxicol.* **2001,** *14* (6), 611-650.
3. Bertz, R. J.; Granneman, G. R. Use of in vitro and in vivo data to estimate the likelihood of metabolic pharmacokinetic interactions. *Clin. Pharmacokinet.* **1997,** *32* (3), 210-258.
4. Cojocaru, V.; Winn, P. J.; Wade, R. C. The ins and outs of cytochrome P450s. *Biochim. Biophys. Acta, Gen. Subj.* **2007,** *1770* (3), 390-401.
5. Rydberg, P.; Rod, T. H.; Olsen, L.; Ryde, U. Dynamics of water molecules in the active-site cavity of human cytochromes P450. *J. Phys. Chem. B* **2007,** *111* (19), 5445-5457.

6. Meunier, B.; de Visser, S. P.; Shaik, S. Mechanism of oxidation reactions catalyzed by cytochrome P450 enzymes. *Chem. Rev.* **2004,** *104* (9), 3947-3980.

7. Shaik, S.; Kumar, D.; de Visser, S. P.; Altun, A.; Thiel, W. Theoretical perspective on the structure and mechanism of cytochrome P450 enzymes. *Chem. Rev.* **2005,** *105* (6), 2279-2328.

8. Kumar, D.; de Visser, S. P.; Sharma, P. K.; Hirao, H.; Shaik, S. Sulfoxidation mechanisms catalyzed by cytochrome P450 and horseradish peroxidase models: Spin selection induced by the ligand. *Biochemistry* **2005,** *44* (22), 8148-8158.

9. Loew, G. H.; Chang, Y. T. Theoretical-Studies of the Oxidation of N-Containing and S-Containing Compounds by Cytochrome-P450. *Int. J. Quantum Chem.* **1993,** 815-826.

10. Sharma, P. K.; de Visser, S. P.; Shaik, S. Can a single oxidant with two spin states masquerade as two different oxidants? A study of the sulfoxidation mechanism by cytochrome P450. *J. Am. Chem. Soc.* **2003,** *125* (29), 8698-8699.

11. Cho, K. B.; Moreau, Y.; Kumar, D.; Rock, D. A.; Jones, J. P.; Shaik, S. Formation of the active species of cytochrome P450 by using iodosylbenzene: A case for spin-selective reactivity. *Chem. Eur. J.* **2007,** *13* (14), 4103-4115.

12. Li, C.; Zhang, L.; Zhang, C.; Hirao, H.; Wu, W.; Shaik, S. Which Oxidant Is Really Responsible for Sulfur Oxidation by Cytochrome P450? *Angew. Chem. Int. Ed.* **2007,** *46* (43), 8168-8170.

13. Afzelius, L.; Arnby, C. H.; Broo, A.; Carlsson, L.; Isaksson, C.; Jurva, U.; Kjellander, B.; Kolmodin, K.; Nilsson, K.; Raubacher, F.; Weidolf, L. State-of-the-art tools for computational site of metabolism predictions: Comparative analysis, mechanistical insights, and future applications. *Drug Metab. Rev.* **2007,** *39* (1), 61-86.

14. Bu, H. Z. A literature review of enzyme kinetic parameters for CYP3A4-mediated metabolic reactions of 113 drugs in human liver microsomes: Structure-kinetics relationship assessment. *Curr. Drug Metab.* **2006,** *7* (3), 231-249.

15. de Montellano, P. R. O.; De Voss, J. J. Oxidizing species in the mechanism of cytochrome P450. *Nat. Prod. Rep.* **2002,** *19* (4), 477-493.

16. Seto, Y.; Guengerich, F. P. Partitioning Between N-Dealkylation and N-Oxygenation in the Oxidation of N,N-Dialkylarylamines Catalyzed by Cytochrome-P450-2B1. *J. Biol. Chem.* **1993,** *268* (14), 9986-9997.

17. Becke, A. D. Density-Functional Thermochemistry .3. the Role of Exact Exchange. *J. Chem. Phys.* **1993,** *98* (7), 5648-5652.

18. Becke, A. D. A New Mixing of Hartree-Fock and Local Density-Functional Theories. *J. Chem. Phys.* **1993,** *98* (2), 1372-1377.

19. Lee, C. T.; Yang, W. T.; Parr, R. G. Development of the Colle-Salvetti Correlation-Energy Formula Into A Functional of the Electron-Density. *Phys. Rev. B* **1988,** *37* (2), 785-789.

20. Vosko, S. H.; Wilk, L.; Nusair, M. Accurate Spin-Dependent Electron Liquid Correlation Energies for Local Spin-Density Calculations - A Critical Analysis. *Canadian Journal of*

Physics **1980,** *58* (8), 1200-1211.

21. Schafer, A.; Horn, H.; Ahlrichs, R. Fully Optimized Contracted Gaussian-Basis Sets for Atoms Li to Kr. *J. Chem. Phys.* **1992,** *97* (4), 2571-2577.

22. Hehre, W. J.; Ditchfield, R.; Pople, J. A. Self-Consistent Molecular-Orbital Methods .12. Further Extensions of Gaussian-Type Basis Sets for Use in Molecular-Orbital Studies of Organic-Molecules. *J. Chem. Phys.* **1972,** *56* (5), 2257-&.

23. Hariharan, P. C.; Pople, J. A. Influence of Polarization Functions on Molecular-Orbital Hydrogenation Energies. *Theor. Chim. Acta* **1973,** *28* (3), 213-222.

24. Francl, M. M.; Pietro, W. J.; Hehre, W. J.; Binkley, J. S.; Gordon, M. S.; Defrees, D. J.; Pople, J. A. Self-Consistent Molecular-Orbital Methods .23. A Polarization-Type Basis Set for 2Nd-Row Elements. *J. Chem. Phys.* **1982,** *77* (7), 3654-3665.

25. Frisch, M. J.; Pople, J. A.; Binkley, J. S. Self-Consistent Molecular-Orbital Methods .25. Supplementary Functions for Gaussian-Basis Sets. *J. Chem. Phys.* **1984,** *80* (7), 3265-3269.

26. Rulisek, L.; Jensen, K. P.; Lundgren, K.; Ryde, U. The reaction mechanism of iron and manganese superoxide dismutases studied by theoretical calculations. *J. Comput. Chem.* **2006,** *27* (12), 1398-1414.

27. Strickland, N.; Harvey, J. N. Spin-forbidden ligand binding to the ferrous-heme group: Ab initio and DFT studies. *J. Phys. Chem. B* **2007,** *111* (4), 841-852.

28. Liao, M. S.; Watts, J. D.; Huang, M. J. Assessment of the performance of density-functional methods for calculations on iron porphyrins and related compounds. *J. Comput. Chem.* **2006,** *27* (13), 1577-1592.

29. Rydberg, P.; Sigfridsson, E.; Ryde, U. On the role of the axial ligand in heme proteins: a theoretical study. *J. Biol. Inorg. Chem.* **2004,** *9* (2), 203-223.

30. Sharp, K. A.; Honig, B. Electrostatic Interactions in Macromolecules - Theory and Applications. *Annu. Rev. Biophys. Biophys. Chem.* **1990,** *19*, 301-332.

31. Honig, B.; Nicholls, A. Classical Electrostatics in Biology and Chemistry. *Science* **1995,** *268* (5214), 1144-1149.

32. Schutz, C. N.; Warshel, A. What axe the dielectric "constants" of proteins and how to validate electrostatic models? *Proteins.* **2001,** *44* (4), 400-417.

33. Klamt, A.; Schuurmann, G. Cosmo - A New Approach to Dielectric Screening in Solvents with Explicit Expressions for the Screening Energy and Its Gradient. *J. Chem. Soc. , Perkin Trans. 2* **1993,** (5), 799-805.

34. Klamt, A.; Jonas, V.; Burger, T.; Lohrenz, J. C. W. Refinement and parametrization of COSMO-RS. *J. Phys. Chem. A* **1998,** *102* (26), 5074-5085.

35. Jensen, F. Introduction to Computational Chemistry. John Wiley & Sons: Chichester, 1999; pp 292-304.

36. Treutler, O.; Ahlrichs, R. Efficient Molecular Numerical-Integration Schemes. *J. Chem. Phys.*

1995, *102* (1), 346-354.

37. Ogliaro, F.; Cohen, S.; de Visser, S. P.; Shaik, S. Medium polarization and hydrogen bonding effects on compound I of Cytochrome p450: What kind of a radical is it really? *J. Am. Chem. Soc.* **2000,** *122* (51), 12892-12893.

38. Baciocchi, E.; Lanzalunga, O.; Pirozzi, B. Oxidations of benzyl and phenethyl phenyl sulfides. Implications for the mechanism of the microsomal and biomimetic oxidation of sulfides. *Tetrahedron* **1997,** *53* (36), 12287-12298.

39. Alvarez, J. C.; Demontellano, P. R. O. Thianthrene 5-Oxide As A Probe of the Electrophilicity of Hemoprotein Oxidizing Species. *Biochemistry* **1992,** *31* (35), 8315-8322.

40. Olsen, L.; Rydberg, P.; Rod, T. H.; Ryde, U. Prediction of activation energies for hydrogen abstraction by cytochrome P450. *J. Med. Chem.* **2006,** *49* (22), 6489-6499.

41. Jones, J. P.; Mysinger, M.; Korzekwa, K. R. Computational models for cytochrome P450: A predictive electronic model for aromatic oxidation and hydrogen atom abstraction. *Drug Metab. Dispos.* **2002,** *30* (1), 7-12.

42. Hay, P. J.; Wadt, W. R. Abinitio Effective Core Potentials for Molecular Calculations - Potentials for K to Au Including the Outermost Core Orbitals. *J. Chem. Phys.* **1985,** *82* (1), 299-310.

43. *Jaguar,* version 7.0; Schrodinger LLC: New York, 2007